

Tendon Sheath Analysis for Estimation of Distal End Force and Elongation

Low Soon Chiang, Phee Soo Jay, *Member, IEEE*, Pietro Valdastrì, *Member, IEEE*, Arianna Menciassi, *Member, IEEE*, Paolo Dario, *Fellow, IEEE*,

Abstract— Tendon sheath actuation can be found in many applications, particularly in robotic hand and surgical robots. Due to friction between the tendon and sheath, many undesirable characteristic such as backlash, hysteresis and non-linearity are present. It is desirable to know the end effector force and elongation of the tendon to control the system effectively, but it is not always feasible to fix sensors at the end effector. A method to estimate the end effector parameters using only a force and position sensor at the proximal site is given. An analytical study is presented and experiments are reported to support the result, showing a max full scale error of approximately 7%. This result is achieved if the shape of the sheath remains the same and buckling is negligible. The results presented in this study could contribute towards haptic development in robotics surgery.

Index Terms—Tendon sheath, cable actuation, surgical robots.

I. INTRODUCTION

Tendon sheath system generally consists of a hollow helical coil wire, acting as a sheath, and an internal cable, that acts as the tendon. When the tendon is pulled at one end, it slides within the sheath, thereby allowing the pulling force to be transmitted to the other end of the sheath. A common example of the tendon sheath actuation is Bowden cable or bicycle brakes. This mode of actuation is useful when it is desired to provide force through a flexible route of transmission and taking up very little space and mass at the end effector. Due to these reasons, tendon sheath actuation has found its way into many applications such as robotic hands and surgical robots [1, 2, 3, 4, 5].

The tendon sheath system however gives out problems such as non-linearity and high friction. Furthermore, it introduces dead zone, hysteresis and direction dependent behavior that is not desirable for control and sensing [6]. Therefore, it is desired to determine both the force output and the elongation of the tendon sheath system to control the end effector

Manuscript received January 15, 2009. This work was supported in part by the National Medical Research Council (Singapore) under Grant NMRC/0827/2004 and Nanyang Technological University (Singapore) under Grant SUG44/04.

Low Soon Chiang and Phee Soo Jay are with the Nanyang Technological University, School of Mechanical and Aerospace Engineering, Robotics Research Center, Blk N3-01a-01, 50 Nanyang Ave, Singapore 639798. (+65-67905568; fax: +65-67935921; e-mail: sclow@ntu.edu.sg, msjphoe@ntu.edu.sg).

Pietro Valdastrì, Arianna Menciassi and Paolo Dario are with CRIM Lab, Scuola Superiore Sant'Anna, viale R. Piaggio 34, 56025 Pontedera (PI), Italy. (e-mail: pietro, arianna, dario @sss.it).

properly. This could enable torque control, force feedback and closed loop positioning. Some studies of tendon sheath actuation on robotic arms managed to achieve joint torque control by introducing sensors at the end effector [7].

However, in the case of robotic system for Natural Orifice Transluminal Endoscopic Surgery (NOTES) [4, 5], placing multiple sensors at the end effector is difficult due to size constraints and high dexterity requirements. For NOTES procedures, the instrument accesses the human body through a natural orifice, i.e. mouth, vagina, or anus. Then it must incise a small hole inside the interior lumen to reach the target site, where the surgery is performed. The endoluminal access prevents scars on the patient's body, thus minimizing the recovery time and hospitalization. Desirable features for NOTES robotic instrumentation are bimanual operation, dexterity, and reduced size. Considering the solutions reported in [4, 5], each arm should have more than three Degrees of Freedom (DOFS), an outer diameter of less than 7 mm, and a flexible body. Providing the end effector with sensors would reduce the range of movement, robustness and force output. Furthermore, the sensors would need to be sterilized prior the surgical intervention, thus introducing a further issue to be considered. The sensors also have to be inert to the different fluids inside the human body to obtain accurate readings.

As such, a novel means of predicting force and elongation of the tendon sheath system at the end effector of an instrument is proposed. The studies made on tendon sheath actuation and the theory behind its application is presented. An experimental approach has been followed and the result for a typical trial is presented. The limitations and possible means to reduce errors are described in the discussion followed by a conclusion at the end of the paper.

II. TENDON SHEATH ANALYSIS

In the following, the sheath is assumed to be bent with a constant radius of curvature as seen in Figure 1. In our model μ is the friction coefficient between the sheath and the tendon, N is the normal force the sheath is exerting on the tendon in this unit length, T is the tension of the tendon, C is the compression force experienced by the sheath, T_{in} is the tension at one end of the sheath, R is the bending radius of the tendon, x is the longitudinal coordinate from the housing end of the sheath to the present location, F is the friction between the tendon and the sheath in this unit length. To simplify our model, μ can be assumed as the dynamic friction when the tendon is moving within the sheaths and it is a constant.

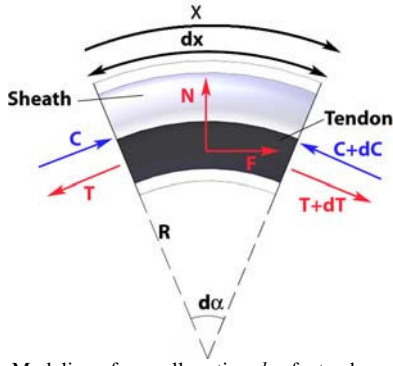


Figure 1: Modeling of a small section dx of a tendon and sheath

Using the force balance equations on the tendon for a small section dx , corresponding to the angle $d\alpha$, we have [6]

$$T d\alpha = -N, d\alpha = dx/R, F = \mu N \text{ and } dT = F$$

thus obtaining

$$\frac{dT}{dx} = -\frac{\mu}{R} T$$

$$T(x) = T_{in} e^{-\frac{\mu}{R}x} \quad (1)$$

Next, the force balance equation is applied on the sheath. Forces N and F for the tendon are equal and opposite to the forces N and F of the sheath since they are reacting against each other. Since the tendon thickness is close to the inner diameter of the sheath and the segment of tendon sheath is significantly small, the angle of both tendon and sheath is assumed to be the same. Therefore we have

$$C = -T, dC = -dT \quad (2)$$

The compressive force measured at the proximal end of the sheath is the same as the tension measured from the tendon at the same end. This result is easily verified by experiments.

The theory presented so far applies only to sheath and tendon with a fixed curvature throughout its length, as shown in Figure 2(i). In general, the sheaths are free to move and the curvature is different throughout the whole length, as shown in Figure 2(ii). This is modeled as a sheath having n sections, each having a different radius of curvature R_1 to R_n and a displacement of x_1 to x_n from the housing. In this case equation (1) becomes

$$T(x) = T_{in} \left(e^{-\frac{\mu}{R_1}x_1 - \frac{\mu}{R_2}(x_2-x_1) - \dots - \frac{\mu}{R_{n-1}}(x_{n-1}-x_{n-2}) - \frac{\mu}{R_n}(x-x_{n-1})} \right) \quad (3)$$

$(x_{n-1} < x < x_n)$

To predict the tension at the end of the sheath, expression (3) can be simplified as

$$T_{out} = T_{in} e^{-K} \quad (4)$$

where

$$K = \mu \left(\frac{x_1}{R_1} + \frac{x_2 - x_1}{R_2} + \dots + \frac{x_n - x_{n-1}}{R_n} \right)$$

represents the effective friction between the tendon and sheath. It is important to note that, if the sheath does not change its shape, K is a constant. It is impossible to determine x_i and R_i , but there is a way to make use of this equation as described in the following.

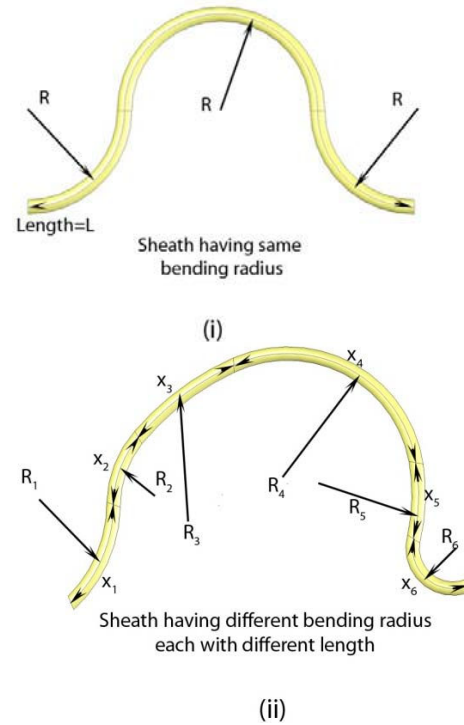


Figure 2: Simplified model of the sheath compared with a generic sheath

Another relevant parameter is the elongation of the tendon and sheath system under a certain force. The study is initially applied to a sheath with a fixed bending radius applying it to a generic sheath. Using e as the tendon elongation and E as the combined stiffness of the tendon and sheath, we have

$$e(x) = \frac{T(x)}{E} \quad (5)$$

where the tendon tension varies with x . To obtain the total elongation, equation (5) must be integrated over the length of the tendon sheath system, thus obtaining

$$e_{total} = \frac{1}{E} \int_0^x T_{in} e^{-\frac{\mu}{R}x} dx \quad (6)$$

This is actually the area under the graph of the tension distribution T divided over the constant E . The analytical solution is

$$e_{total} = \frac{T_{in}R}{E\mu} \left(1 - e^{-\frac{\mu}{R}x} \right) \quad (7)$$

Another expression is

$$e_{total} = \frac{R}{E\mu} (T_{in} - T_{out}) \quad (8)$$

T_{out} is the tension experienced by the tendon at the end effector. This result is slightly different from the other works reported in literature [6, 7] for two main reasons. First, pretension is not required. Second, it does not make the assumption that the force is evenly distributed within the sheath. When the system is used, it starts with zero or low pretension. In this case, two actuators are used to control one DOF instead of the traditional one actuator per DOF. This also

simplifies the modeling of the problem, since only one tendon undergoes a tension at any given time.

The above derivation is used when both the tendon and sheath have a constant bending radius. If the sheath is modeled as having n sections, each having a different radius of curvature R_1 to R_n and each having a displacement of x_1 to x_n , then

$$e_{o1} = \frac{R_1}{E\mu} (T_{in} - T_{o1})$$

$$e_{o1} = \frac{T_{in} R_1}{E\mu} \left(1 - e^{-\frac{\mu}{R_1} x_1} \right) \quad (x=x_1) \quad (9)$$

Where e_{o1} is the elongation at $x=x_1$ and T_{o1} is the tension at $x=x_1$. Similarly

$$e_{o2} = \frac{T_{in}}{E\mu} \left[R_1 \left(1 - e^{-\frac{\mu}{R_1} x_1} \right) + R_2 e^{-\frac{\mu}{R_1} x_1} \left(1 - e^{-\frac{\mu}{R_2} (x_2 - x_1)} \right) \right] \quad (x=x_2)$$

$$\dots$$

$$e_{total} = \frac{T_{in}}{E\mu} \left[R_1 \left(1 - e^{-\frac{\mu}{R_1} x_1} \right) + \sum_{i=2}^n R_i e^{-\mu \sum_{j=1}^i \frac{(x_{j-1} - x_{j-2})}{R_{j-1}}} \left(1 - e^{-\frac{\mu}{R_i} (x_i - x_{i-1})} \right) \right] \quad (x=x_n) \quad (10)$$

$$e_{total} = M_e T_{in} \quad (11)$$

Where

$$M_e = \frac{1}{E\mu} \left[R_1 \left(1 - e^{-\frac{\mu}{R_1} x_1} \right) + \sum_{i=2}^n R_i e^{-\mu \sum_{j=1}^i \frac{(x_{j-1} - x_{j-2})}{R_{j-1}}} \left(1 - e^{-\frac{\mu}{R_i} (x_i - x_{i-1})} \right) \right]$$

M_e represents the effective elongation constant of the tendon sheath system. It is a constant if the shape of the tendon and sheath remains the same.

The relationship of K and M_e with T_{in} is expressed in Figure 3. The full line curve represents the actual tension distribution for a generic sheath at T_{in} . The dotted line represents the approximate solution coming from equation (4) as displacement x increases. The value of M_e is proportional to the area under the straight line curve and it is an indication of sheath deformation. In the experimental setup section, the approach to find K and M_e is discussed in detail. It should be noted that just the approximated values for the force at the two ends are relevant for control.

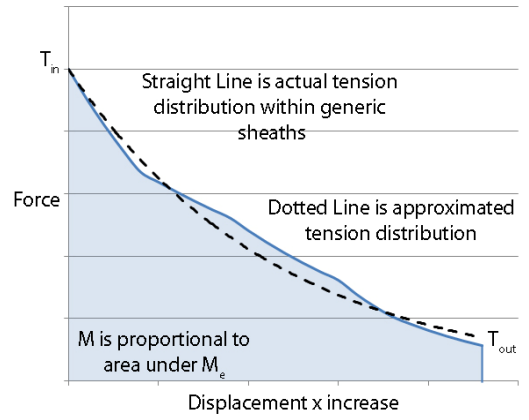


Figure 3: Graphical representation of M_e and K

By approximating the original curvature to the one characterized by K , the relationship between M_e and K can be retrieved by evaluating the area underneath $T_{in}e^{-Kx}$ multiplied by $1/E$,

$$M_e T_{in} = \frac{T_{in} L}{EK} (1 - e^{-K}) \quad (12)$$

$$e^{-K} = -\frac{M_e E}{L} K + 1 \quad (13)$$

It is seen that M_e and K are dependent on each other and the value of M_e is enough to approximate K and vice versa. E is the Young's modulus or stiffness of the tendon and therefore is the same regardless of the shape. There is no readily available solution for equation (13) and numerical methods, such as Newton-Raphson or the Golden Section method have to be used.

However, this result is relevant only when the system undergoes a pulling phase. In the case the tendon is just released after being pulled, the system does not immediately go into the release phase. It undergoes a transitional phase from pulling to releasing.

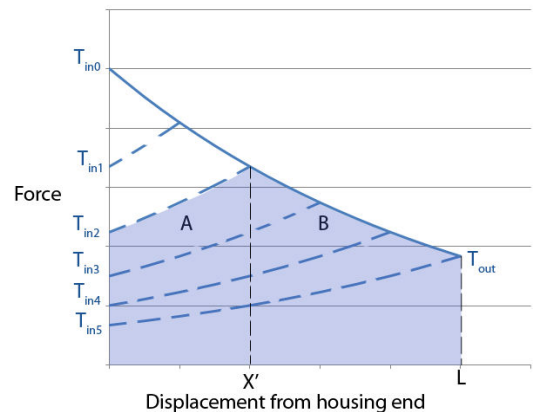


Figure 4: Gradually reducing T_{in} and the tension distribution within the sheath

Figure 4 shows the tension distribution within the sheath as the housing force is gradually reduced. The first effect of a decrease in T_{in} is a reduction of the tension within the sheath, while the tension at the end effector is not affected. Let X' be the distance from the proximal end where the highest amount of tension within the sheath. As T_{in} decreases, X' moves

further from the proximal end and closer to the end effector. Only when X' reaches the end of the sheath, then T_{out} starts to decrease. This is the so called “backlash” of the tendon sheath system.

During the transitional phase, T_{out} remains constant until T_{in} reduces to T_{in5} , as shown in Figure 4. Therefore

$$T_{out} = T_{in0} e^{-K} \quad (14)$$

where T_{in0} is the highest value of the tension recorded at the housing before it starts to loosen.

Differently from tension, the elongation varies during the transitional period. The area under the tension distribution curve is proportional to the elongation of the tendon and sheath and it undergoes relevant variations. This change in the area is observed under the shaded graph of Figure 4.

The elongation of the tendon during the transitional phase is derived in two steps. First, the displacement X' is calculated. The second step is to evaluate the elongation under the shaded areas A and B of the curve. To perform this step, we take advantage from the curvature approximated by K .

Using L as the length of the whole sheath,

$$T_{in} e^{\frac{K}{L} X'} = T_{in0} e^{-\frac{K}{L} X'} \quad (15)$$

$$X' = \frac{L}{2K} \ln \frac{T_{in0}}{T_{in}} \quad (16)$$

When $X'=L$, $T_{in}=T_{in0}e^{-2K}$ is the force that the tension at the housing side has to release before T_{out} reduces. This value can be calculated and used online in order to infer if the system is still working within the backlash region.

Now a way to calculate the elongation coming from area A of Figure 4 is presented. Using A be the area underneath the tension distribution from $x=0$ to $x=X'$,

$$\begin{aligned} \text{Area } A &= \int_0^{X'} e^{\frac{K}{L} x} dx \\ \text{Area } A &= \frac{L}{K} \left(1 - e^{-\frac{K}{L} X'} \right) \end{aligned} \quad (17)$$

Similar to the derivation of equation (6), the elongation under Area A is given by the area of the curve multiplied by the highest tension in A , divided by E . In this case, the highest tension within A is $T_{in} e^{\frac{K}{L} X'}$. The resulting equation becomes

$$e_A \approx \frac{T_{in} L e^{\frac{K}{L} X'}}{EK} \left(1 - e^{-\frac{K}{L} X'} \right) \quad (18)$$

The elongation caused by area B is proportional to the area under the curve from $x=X'$ to $x=L$.

$$\text{Area } B = \frac{L}{K} \left(1 - e^{-\frac{K}{L}(L-X')} \right)$$

$$e_B \approx \frac{T_{in} L e^{\frac{K}{L} X'}}{EK} \left(1 - e^{-K \left(1 - \frac{X'}{L} \right)} \right) \quad (19)$$

The combined elongation for the two areas become

$$e_{total} \approx \frac{T_{in} L}{EK} \left(2e^{\frac{K}{L} X'} - 1 - e^{-K \left(1 - \frac{2KX'}{L} \right)} \right) \quad (20)$$

By substituting $X' = \frac{L}{2K} \ln \frac{T_{in0}}{T_{in}}$ into the equation above,

we obtain

$$e_{total} \approx \frac{L}{EK} \left(2\sqrt{T_{in0} T_{in}} - T_{in} - T_{in0} e^{-K} \right) \quad (21)$$

Deriving it in a similar fashion, the force approximation when the system is at the releasing phase is

$$T_{out} = T_{in0} e^K \quad (22)$$

while the elongation is

$$e_{out} = M T_{in} e^K \quad (23)$$

and the force prediction at the transitional phase from release to pull is

$$T_{out} = T_{in0} e^{-K} \quad (24)$$

Finally, the elongation during the transitional phase from release to pull is

$$e \approx \frac{L}{EK} \left[T_{in} - 2\sqrt{T_{in} T_{in0}} + T_{in0} e^K \right] \quad (25)$$

III. EXPERIMENTAL SETUP

In order to verify the theoretical aspects derived in the previous section as well as to determine the accuracy of the estimation, the experimental setup shown in Figure 5 is used.

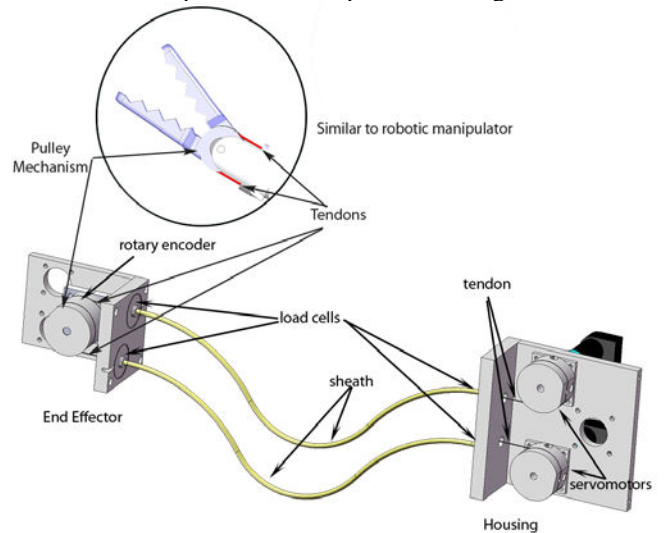


Figure 5: A schematic representation of the experimental setup

At the housing, or proximal end, two Faulhaber 2642W024CR DC servomotors with a gear head of 30/1S 134:1 ratio are fixed. The two tendons for controlling one

DOF are fixed to the two actuators separately. These actuators are set to position control and each of them takes advantage from a rotary optical encoder HEDS-5540 A14 to measure the angular rotation. The combined resolution of the encoder with the gear head is 67000 lines per revolution. At the end effector side, or distal end, another actuator is used under torque control. Its main purpose is to simulate the load that the end effector exerts on the environment. It also has the same rotary encoder attached to the actuator to measure the amount of movement made by the system. In the middle, two tendons and sheaths are used together with an overtube to prevent the buckling effect. The forces at both ends of the system are measured with donut shaped load cells LW-1020 from Interface. Although they measure the compression experienced by the sheaths instead of the tension from the tendons, the results are similar to measuring the tension force at the same end, as shown in equation (2). The elastic modulus of the tendons is known beforehand either from the supplier or measured with a simple stiffness test.

The rationale of using two actuators for a single DOF is to ensure only one tendon is providing a tension at a given time while the antagonistic tendon is left loose. This provides the highest possible force from the tendon, since it does not have to work against the other taut antagonistic tendon.

After the end effector reaches the site where it is designated to work, the global shapes of the tendon and sheath are fixed. The experimental procedure then proceeds as follows. First, it is necessary to determine the values of K and M_e for this particular shape of the sheaths. To do so, initialization is required. The actuator at one end of the DOF pulls one end of the tendon until the slave reaches the end of its motion. This is the point where further pulling of the tendon at one side of the joint does not change the rotation angle, as shown in Figure 6. Regarding the actuator at the other side of the DOF, it must minimize the pulling force to prevent interference with the initialization procedure. This is possible since it is controlled by a separate actuator and it reads the load cell on its side, thus deciding either to pull or release the tendon accordingly.

Even when the joint at the distal end reaches the limit of its motion, the actuator at the pulling side still continues to pull in the tendon at the proximal end. At this point in time, the reading of the force at the proximal loadcell start to increases as the tendon pulls harder and harder at the joint that has reached its motion limit. Therefore the system knows when the joint had reached its motion limit without the need of an encoder. This length that is pulled from the proximal actuator with its encoder at this point is the amount of deformation of the tendon within the sheath and e_{out} can be known. Using equation (11),

$$M_e = \frac{e_{out}}{T_{in}}$$

e_{out} is obtained from the encoder reading, while T_{in} is the force obtained from the load cell of the pulling side at the proximal end. The value of M_e is derived from the process of initialization, while K is obtained from equation (12).

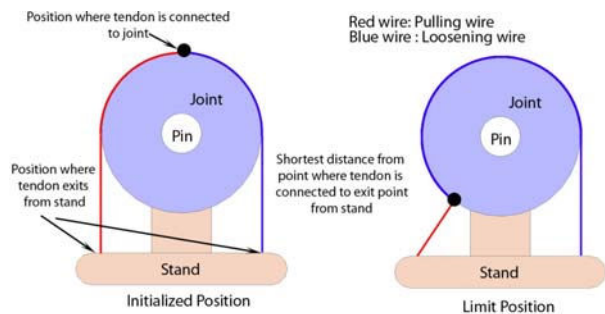


Figure 6: Limit of motion for a simple revolute joint

With these two values, the elongation and force at the distal end could be approximated, since both elongation and force at the distal end are a simple function of T_{in} . This is repeated for the opposite direction of the DOF as well to capture the specific value of M_e and K . During initialization, the user must not let the end effector touches any object in the environment. After initialization, the user can start to use the master slave robotic system as desired and both the end effector force and the elongation is computed using the derived K and M_e values.

An assumption is made regarding the use of constant values for K and M_e . After the system has reached the target site, the user no longer moves the sheaths around and the shape of the sheaths is assumed to be fixed. In this condition, constant values for K and M_e can be used with negligible position and force errors. In the case the user needs to change the system position, then the robotic system require a quick initialization to compute the new values for K and M_e before it is used.

IV. EXPERIMENTAL RESULT

First of all, the setup is initialized to obtain K and M_e . The experiment is then performed with three profiles as shown in Figure 7. In the first profile, the actuator pulls the tendon until it reaches a limited force of approximately 20N on the housing. In the second phase, the tendon is released at the housing to about 5N, while in the third phase, the tendon is pulled again back to 20N. These last two steps test the pull-to-release, release, release-to-pull and pulling phases and check the approximation level with the actual reading. In Figure 7, the curves on the left are the readings from the housing load cell while the dotted curves on the right are the readings from the end effector load cell.

The comparison of the end effector force with the predicted force is shown in Figure 8. The results are broken up into three phases. The graphs on the left are the plots of actual vs. predicted end effector force, while the graphs on the right are the actual vs. predicted elongation plots. The continuous lines in full are the actual sensed values, while the dotted lines are the predicted values.

For this experiment, the maximum full scale error is approximately 7%, while for the elongation, it is approximately 3%. The higher error in the force reading is due to the fact that the value of M_e is found and then used to deduce K . Overall the average full scale error is less than 2%.

V. DISCUSSION

Although this method is capable of sensing both the elongation and end effector force, it can be used only in the case where there is little or no change in the sheath shape after initialization. The greater the shape of the sheath changes, the worse the estimation becomes. If a great change of the shape of the sheath is suspected, it is recommended to reinitialize the system again to obtain updated values for M_e and K . If the application force on the sheath undergoes regular displacements, then this method should not be used. However, if the application is not critical and does not require high accuracy, then small changes in the shape of the sheaths during usage can be tolerated.

The force predicted at the end effector is already the combined force the joint experienced. Therefore, it can directly be scaled to the master controller without the need of any further calculation or conversion.

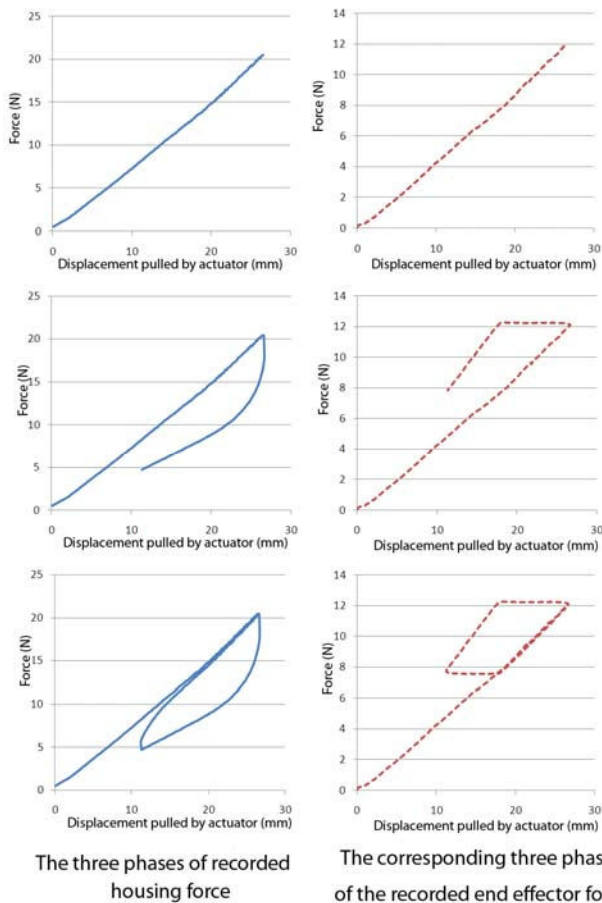
This method can also be used for predicting the end effector parameters for any robotic arm having relatively constant sheath shapes. This offers an additional advantage of locating the sensors away from the end effector. This can reduce the inertia of the end effector and allow the hand to work in extreme environmental conditions, whereby sensors at the end effector would fail.

VI. CONCLUSIONS

The mathematical modeling of the tendon and sheath for the force at the end of the sheath, as well as overall elongation, are described in the paper. Using the analytical approach, important values such as K and M_e for predicting end effector force and elongation are identified. The method to find these values is explained and the results are verified experimentally. Using this method, the end effector force and elongation is predicted without a sensor attached. The required assumptions and important considerations to take note of are also given in the discussion section.

REFERENCES

- [1] F. Lotti, P. Tiezzi, G. Vassura, L. Biagiotti, G. Palli, C. Melchiorri; *Development of UB Hand 3: Early Results*; Proc. IEEE Int. Conf. on Robotics and Automation; Barcelona, Spain; April 2005
- [2] Z.H. Sun; G. Bao; Q.J. Yang; Z.W. Wang; *Design of a Novel Force Feedback Dataglove Based on Pneumatic Artificial Muscles*; Proc. 2006 IEEE Int. Conf. Mechatronics and Automation; Luoyang, China; June 2006
- [3] A. Caffaz, G. Cannata; *The Design and the Development of the DIST-Hand Dextrous Gripper*; Proc. IEEE Int. Conf. Robotics and Automation; Leuven, Belgium; May 1998
- [4] S.J. Phee, S.C. Low, Z.L. Sun, K.Y. Ho, W.M. Huang, Z.M. Thant; *Robotic System for No-Scar Gastrointestinal Surgery*; Int. Journal of Med. Rob. And Comp. Assisted Sur.; Vol. 4; PP 15-22
- [5] D. J. Abbott, C. Becke, R.I. Rothstein, W.J. Peine; *Design of an Endoluminal NOTES Robotics System*; Proc. IEEE/RSJ Int. Conf. on Intelligent Robots and Systems; San Diego, CA, USA; Nov 2007
- [6] M. Kaneko, T. Yamashita, K. Tanie; *Basic Considerations for Tendon Drive Robots*; Int. Conf. Advanced Robotics; Pisa, Italy; June 91
- [7] G. Palli, C. Melchiorri; *Model and Control of Tendon-Sheath Transmission Systems*; Proc. IEEE Int. Conf. Robotics and Automation; Orlando, Florida; May 2006



The three phases of recorded housing force

The corresponding three phases of the recorded end effector force

Figure 7: The phases of pulling and releasing that is studied

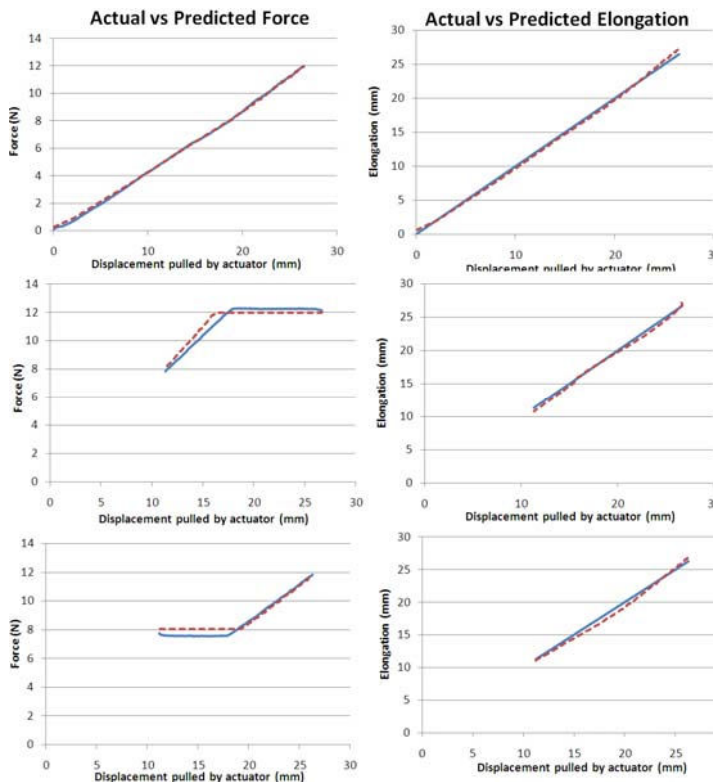


Figure 8: The result of the actual force/elongation vs. predicted force/elongation